Photonic lantern adaptive spatial mode control in LMA fiber amplifiers using SPGD**

Juan Montoya[1,*], Chris Aleshire[1], Christopher Hwang[1], Nicolas K. Fontaine[2], Amado Velazquez[3], Dale H. Martz[1], T.Y. Fan[1], and Dan Ripin[1]

[1]MIT Lincoln Laboratory, 244 Wood St., Lexington, MA 02420, USA
[2]Bell Laboratories, Alcatel-Lucent, 791 Holmdel Rd., Holmdel, N.J. 07733, USA
[3]CREOL, The College of Optics and Photonics, the University of Central Florida, Orlando, FL 32816, USA
[*]juan.montoya@ll.mit.edu

Abstract: We demonstrate adaptive-spatial mode control (ASMC) in few-moded double-clad large mode area (LMA) fiber amplifiers by using an all-fiber based photonic lantern. Three single-mode fiber inputs are used to adaptively inject the appropriate superposition of input modes in a multimode gain fiber to achieve the desired mode at the output. By actively adjusting the relative phase of the single mode inputs, near unity coherent combination resulting in a single fundamental mode at the output is achieved.

OCIS codes: (140.3510) Lasers, fiber; (140.3425) Laser stabilization; (060.2340) Fiber optics components; (110.1080) Active or adaptive optics;

References and links

1. C. Jauregui, J. Limpert, and A. Tünnermann, "High Power Fibre Lasers," Nat. Photonics 7, 861 (2013).
2. C. X. Yu, S. J. Augst, S. M. Redmond, K. C. Goldizen, D. V. Murphy, A. Sanchez, and T. Y. Fan, "Coherent combining of a 4 kW, eight-element fiber amplifier array," Opt. Lett. **36**, 2686-2688 (2011).
3. F. Jansen, F. Stutzki, H. Otto, T. Eidam, A. Liem, C. Jauregui, J. Limpert, and A. Tünnermann, "Thermally induced waveguide changes in active fibers," Opt. Express **20**, 3997-4008 (2012).
4. T. Eidam, C. Wirth, C. Jauregui, F. Stutzki, F. Jansen, H. Otto, O. Schmidt, T. Schreiber, J. Limpert, and A. Tünnermann, "Experimental observations of the threshold-like onset of mode instabilities in high power fiber amplifiers," Opt. Express **19**, 13218-13224 (2011).
5. A. V. Smith and J. J. Smith, "Mode instability in high power fiber amplifiers," Opt. Express **19**, 10180-10192 (2011).
6. S. G. Leon-Saval, T. A. Birks, J. Bland-Hawthorn, and M. Englund, "Multimode fiber devices with single-mode performance," Opt. Lett. **30**, 2545-2547 (2005).
7. D. Noordegraaf, P. M. Skovgaard, M. D. Nielsen, and J. Bland-Hawthorn, "Efficient multi-mode to single-mode coupling in a photonic lantern," Opt. Express **17**, 1988-1994 (2009).
8. S. G. Leon-Saval, A. Argyros, and J. Bland-Hawthorn, "Photonic lanterns: a study of light propagation in multimode to single-mode converters," Opt. Express **18**, 8430-8439 (2010).
9. N. K. Fontaine, Roland Ryf, J. Bland-Hawthorn, and S. G. Leon-Saval, "Geometric requirements for photonic lanterns in space division multiplexing," Opt. Express **20**, 27123-27132 (2012).
10. R. J. Black, L. Gagnon, *Optical Waveguide Modes: Polarization, Coupling and Symmetry* (New York, NY, USA: McGraw-Hill, 2009).
11. D. A. B. Miller, "All linear optical devices are mode converters," Opt. Express **20**, 23985-23993 (2012).
12. S. M. Redmond, D. J. Ripin, C. X. Yu, S. J. Augst, T. Y. Fan, P. A. Thielen, J. E. Rothenberg, and G. D. Goodno, "Diffractive coherent combining of a 2.5 kW fiber laser array into a 1.9 kW Gaussian beam," Opt. Lett. **37**, 2832-2834 (2012).
13. W. B. Veldkamp, J. R. Leger, and G. J. Swanson, "Coherent summation of laser beams using binary phase gratings," Opt. Lett. **11**, 303-305 (1986).
14. T. Y. Fan, "The effect of amplitude (power) variations on beam combining efficiency for phased arrays," IEEE J. Sel. Top. Quantum Electron. **15**(2), 291–293 (2009).
15. G. D. Goodno, C. Shih, and J. E. Rothenberg, "Perturbative analysis of coherent combining efficiency with mismatched lasers," Opt. Express **18**, 25403-25414 (2010).
16. M. A. Vorontsov, G. W. Carhart, and J. C. Ricklin, "Adaptive phase-distortion correction based on parallel gradient-descent optimization," Opt. Lett. **22**, 907-909 (1997)
17. J. Montoya, S. J. Augst, K. Creedon, J. Kansky, T. Y. Fan, and A. Sanchez-Rubio, "External cavity beam combining of 21 semiconductor lasers using SPGD," Appl. Opt. **51**, 1724-1728 (2012).

**This work is sponsored by the HEL-JTO under Air Force Contract #FA8721-05-C-0002. Opinions, interpretations, conclusions and recommendations are those of the author and are not necessarily endorsed by the United States Government.

18. H. Otto, C. Jauregui, F. Stutzki, F. Jansen, J. Limpert, and A. Tünnermann, "Controlling mode instabilities by dynamic mode excitation with an acousto-optic deflector," Opt. Express **21**, 17285-17298 (2013).
19. D. Flamm, D. Naidoo, C. Schulze, A. Forbes, and M. Duparré, "Mode analysis with a spatial light modulator as a correlation filter," Opt. Lett. **37**, 2478-2480 (2012).
20. C. Schulze, D. Flamm, S. Unger, S. Schröter, and M. Duparré, "Measurement of higher-order mode propagation losses in effectively single mode fibers," Opt. Lett. **38**, 4958-4961 (2013).
21. C. Schulze, R. Brüning, S. Schröter, and M. Duparré, "Mode Coupling in Few-Mode Fibers Induced by Mechanical Stress," J. Lightwave Technol. **33**, 4488-4496 (2015).
22. T. A. Birks, B. J. Mangan, A. Díez, J. L. Cruz, and D. F. Murphy, "“Photonic lantern” spectral filters in multi-core fibre," Opt. Express **20**, 13996-14008 (2012).

1. Introduction

Fiber amplifier power scaling has shown significant progress as evidenced by the commercial availability of kW-class amplifiers [1]. Power scaling beyond the kW-class has been achieved by coherently combining several fiber amplifiers [2]. One of the benefits of coherent beam combination (CBC) arises from aperture synthesis. A larger aperture, with less power per unit area, is achieved through synthesis of several subapertures. Scaling the modal area of an individual fiber amplifier similarly serves to reduce the peak intensity. The lowering of the intensity through modal-area scaling by utilization of large mode area (LMA) fibers has suppressed a number of nonlinearities, which has resulted, in part, in the successful power scaling of today’s fiber amplifiers. However, advances achieved by scaling the modal area of an individual fiber amplifier have been hampered by the onset of multi-mode instability (MMI) [3-5]. Conventional means to maintain single-mode operation in LMA fibers by reducing the higher-order mode content through coiling has been limited by the thermally induced nonlinearities that lead to coupling and power transfer amongst the modes.

Here an alternative approach to spatial-mode control using active feedback is described. Our results demonstrate the ability of active feedback to stabilize the fundamental mode output of a multimode fiber by appropriately launching the correct superposition of input modes in both phase and amplitude to achieve the desired mode on the output. In effect, an all-fiber based adaptive-optic system is demonstrated that preconditions the input to achieve a nearly diffraction-limited, single-mode beam on the output.

We call this adaptive spatial mode control (ASMC). This all-fiber based adaptive optic approach makes use of photonic lantern technology, which has found applications in astrophotonics [6-8] and spatial-division multiplexing for communications [9]. Below the salient features of the photonic lantern relevant to fiber power scaling is described.

The operation of the combiner is perhaps best described by considering the problem in reverse. Consider launching the fundamental LP01 mode in reverse, labeled u_1 in Fig. 1, into the output of a three-moded photonic lantern. The output fiber illustrated in red in Fig. 1 is referred to as the delivery fiber and may be passive, active, or both (i.e. a passive splice onto an active fiber). For an ideal lossless lantern, properly mode-matched to the delivery fiber, all of the power would be distributed among the input fibers with amplitude v_i and phase θ_i. In order to faithfully reproduce the desired output mode u_1 in the forward direction, the control system must launch the same amplitudes v_i and conjugate phases θ_i on the input.

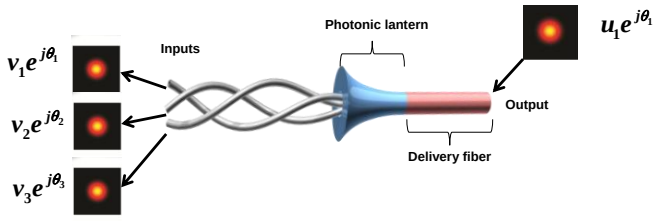

Fig. 1. Instructional schematic of a photonic lantern operating in reverse. The fundamental LP01 mode is launched into the output generating an amplitude and phase distribution among the input fibers. Time-reversal symmetry allows launching the conjugate inputs to reproduce the output.

To gain further insight into the operation of the photonic lantern, one may consider launching a single mode into an individual input fiber as illustrated in Fig. 2. As the input fiber undergoes an adiabatic taper the output emerges as a superposition of output modes u_1, u_2, and u_3 representing the LP01, $LP11_o$, and $LP11_e$ modes respectively. Mathematically, we observe that this input basis [v_1, 0, 0] vector is not the appropriate basis vector to launch on the input to achieve the desired output mode [u_1, 0, 0]. Since the photonic lantern performs a unitary operation, there exists an appropriate set of orthogonal input vectors, which will map onto a desired orthogonal set of output vectors.

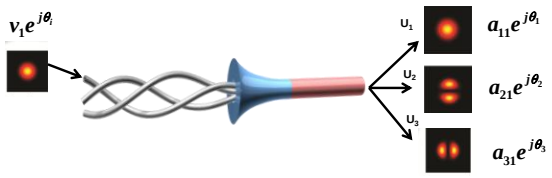

Fig. 2. Launching a single input on one of the input channels in a three-mode lantern results in a superposition of the three modes supported by the delivery fiber. The input and output relation may be described by a transfer matrix.

Moreover, since the photonic lantern is a linear-optical device, it may be considered a mode converter that maps input orthogonal sets to output orthogonal sets [10]. In particular, a transfer matrix may describe the relation between the input and output in a photonic lantern. This relationship between the input and output superposition of modes in an ideal lantern may be compactly expressed as $Av_i = u_i$, where the transfer matrix A may be derived from symmetry considerations [9,10] and is expressed

$$A = \begin{bmatrix} \frac{1}{\sqrt{3}} & \frac{1}{\sqrt{3}} & \frac{1}{\sqrt{3}} \\ -\frac{1}{\sqrt{6}} & -\frac{1}{\sqrt{6}} & \frac{2}{\sqrt{6}} \\ \frac{1}{\sqrt{2}} & -\frac{1}{\sqrt{2}} & 0 \end{bmatrix}. \qquad (1)$$

For the ideal lantern transfer matrix, we observe that launching $[1\ 1\ 1]/(3^{1/2})$ on the input would result in exciting the pure LP01 fundamental mode u_1. An orthogonal input vector $[1\ 1\ -2]/(6^{1/2})$ would excite the u_2 ($LP11_o$) mode, and a third orthogonal input vector $[1\ -1\ 0]/(2^{1/2})$ would excite the u_3 ($LP11_e$) mode.

In practice, fabrication tolerances of a photonic lantern and mode mismatch in the splicing of the lantern to an output fiber, along with any static or dynamic mode coupling in the delivery fiber, would result in a different transfer matrix from the ideal. In addition, loss may result from mode-mismatch between the lantern and the delivery fiber. Nonetheless, in general there is still a suitable input vector to completely excite the desired output mode albeit with some loss [11]. In the most general case, the transfer matrix may then be decomposed using singular value decomposition into the form $Av_i = \sigma_i u_i$, where σ_i represents the transmission loss in exciting mode u_i [9].

2. Photonic Lantern Based Beam Combining

In many respects, a photonic lantern may be viewed as an all-fiber based approach to achieve CBC. For illustration, we compare a diffractive-optical element (DOE) based combining approach [12,13] to a photonic-lantern combiner in Fig. 3. On the left, we observe that sending in a single beam on the input to a DOE results in 3 non-overlapping (orthogonal)

beams on the output. Similarly, sending in a single fiber on the input to a lantern results in three orthogonal beams on the output. It is possible to reverse the DOE operation by sending in three appropriately phase-adjusted beams on the input to achieve a single beam on the output [12]. Similarly, sending in the appropriately phased modes on the input to a photonic lantern results in a fundamental mode on the output.

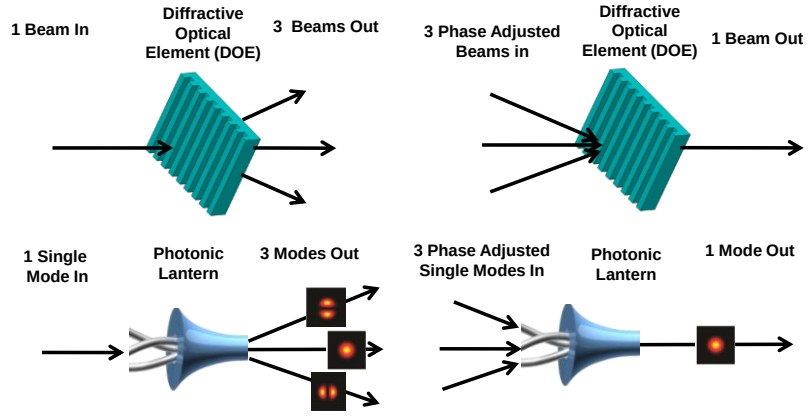

Fig. 3. Comparison of DOE-based coherent beam combining with a photonic-lantern-based beam combining approach. (Upper left) a single beam incident on a 3-channel DOE generates three output beams. (Lower left) a single channel on a photonic lantern generates three modes. (Upper right) three appropriately phased beams incident on a DOE generate a single output beam. (Lower right) three appropriately phased beams incident on a lantern generate a single mode.

This correspondence between the photonic lantern and conventional CBC allows application of the CBC formalism to estimate the impact of various errors on combining efficiency [14-15]. In particular, one can determine the impact of phase, amplitude, and polarization errors on the combining efficiency. The combining efficiency is defined here as the fraction of power in the desired fundamental mode over the total power.

It should be noted that while general CBC principles apply, the photonic lantern also allows for compensation of both static and dynamic mode coupling in the delivery fiber. In this regard, the photonic lantern is analogous to tiled-aperture phased-array CBC in which the input phase and amplitude may be adjusted dynamically to compensate for atmospheric disturbances. The lantern has the advantage in that the number of guided modes in the delivery fiber is finite and known *a priori*. In this respect, the number of input channels must match the number of modes in the delivery fiber for complete compensation.

For the three-channel photonic lantern, it is clear from the matrix description that all three channels are required to purely excite the fundamental mode. In the most general case, N input fibers are needed to efficiently excite the fundamental mode in an N channel fiber [5-9]. Assuming for simplicity the ideal transfer matrix, which requires equal amplitudes on the input to excite the fundamental mode, the impact of the amplitude variation on combining efficiency is

$$\eta = \frac{1}{N} \frac{\left| \sum_{m=1}^{N} \sqrt{P_m} \exp(j\theta_m) \right|}{\sum_{m=1}^{N} P_m} \quad , \qquad (2)$$

where P_m is the power in channel m, and N=3 for the three channel lantern [14]. In the limit of small amplitude errors, the combining efficiency loss ($1-\eta$) is given by $\frac{1}{4}(\sigma_P^2)/P^2$ where P is the nominal power per channel and σ_P is the power standard deviation on the input channels.

Similarly, the RMS phase-variation impact on combining efficiency may be expressed as $(1-\eta)\sim\sigma_\theta^2$ for small phase errors where σ_θ is the RMS phase error.

While the photonic lantern is similar in many respects to other CBC approaches, it offers a number of unique benefits when used in a fiber amplifier. First, the photonic lantern may be integrated (spliced) onto the front-end of a fiber amplifier. Since the photonic lantern is used at the seeding stage, the efficiency of a high-power fiber amplifier is minimally impacted by the insertion loss of the photonic lantern, and, therefore is more forgiving than the insertion loss of a combiner used on the output of a high-power system. Furthermore, the photonic lantern provides a path to modal-area scaling. The scaling recipe simply requires that the number of input fibers match the number of modes in the delivery fiber. Modal-area scaling in turn allows one to suppress intensity-dependent nonlinearities. Lastly, mode control offers the promise of combating MMI and serves as an alternative to or can be used in conjunction with coiling a fiber to provide modal discrimination.

It is worth noting that other active-mitigation strategies to combat MMI have been successfully applied [18]. These alternate approaches have utilized acousto-optic deflection of an incident beam on a fiber. By laterally offsetting the input launch, a different superposition of modes is launched into the gain fiber. Our photonic-lantern ASMC approach differs from the acousto-optic modulator approach in three main aspects: (a) the input is all fiber-based and no free-space optics are needed, (b) the intrinsic mode matching allows one to selectively excite any desired mode with high efficiency, and (c) scaling to large number of modes can be done by simply increasing the number of input fibers.

3. Experimental Results

A proof of concept experiment is illustrated in Fig. 4 below. A seed laser is split into three fibers using a polarization-maintaining fiber splitter. The three output fibers from the splitter are then sent to individually addressable lithium niobate phase modulators. The fiber outputs of the phase modulators are then spliced into a photonic lantern that is mode matched to a delivery fiber consisting of a passive Nufern 25/400 fiber spliced onto an active Yb-doped Nufern 25/400 double-clad fiber. The active fiber is diode pumped using a Dilas 30 W pump module (not shown) that is co-pumped using a 6x1+1 combiner, which serves to combine the seed signal and the pump light to the double-clad gain fiber.

The individual input amplitudes in the photonic lantern were set to be equal. The output of the photonic lantern contribution to the fundamental mode in the passive section of the delivery fiber was observed prior to splicing onto the gain fiber. Based on the observed amplitude variations on the output for equal amplitude launch on the input we estimate a combining loss of ~3%. For an ideal delivery fiber, absent mode-coupling dynamics, dynamic amplitude control is not required, as the delivery fiber would have a static identity transfer matrix. In the presence of mode-coupling dynamics, leading to a temporally varying transfer matrix, amplitude control would generally be required for high efficiency as the overall system transfer matrix would be a product of the lantern transfer matrix with that of the delivery fiber. The impact of amplitude errors on the combining efficiency may be estimated through eq. 2 based on the particular time-varying disturbance. For example, the impact of non-uniform coefficients in the first row of the transfer matrix of eq. 1 may be modeled equivalently as being similar to having uniform coefficients with unequal inputs allowing application of eq. 2. The reason that amplitudes can be set to be near equal and that no dynamic control is needed in this experiment implies that the lantern is near ideal and mode coupling in the delivery fiber is minimal.

The three-channel photonic lantern was fabricated using a similar tapering process to that described in detail elsewhere [7-9]; we briefly review the fabrication process. Three single-mode fibers are placed into a capillary tube. The input fibers are tapered until the fiber modes become guided by their cladding which adiabatically becomes the core of the output fiber, and the capillary tube becomes the new cladding of the output fiber. The index of the capillary tube and the individual fiber claddings determine the index contrast of the output waveguide and are choosen to match the numerical aperture NA of the delivery fiber. The final core size

is also designed to mode-match the delivery fiber, which consists of a 0.065 NA, 25-micron core. The measured insertion loss of each individual fiber into the core of the delivery fiber was less than 3 dB.

A stochastic parallel gradient descent (SPGD) algorithm [16] was used to adaptively determine the appropriate phase to be applied to the input fibers to maximize the on-axis intensity of the output beam. SPGD has been successfully applied to a number of CBC demonstrations [2,12,17]. For completeness, we briefly summarize the operation of the algorithm. The desired fundamental mode is the only mode that contains an on-axis component while the $LP11_e$ and $LP11_o$ modes have an on-axis null. A pinhole is placed before the SPGD detector in order to sample the on-axis (or LP01) component of the output beam. The SPGD controller applies a dither vector across the three phase modulators, although only two phase modulators are actually needed, as the common phase need not be controlled. The same dither vector is then applied with the opposite sign. Based on the response to the applied dithers, a correction is applied to maximize the signal on-axis. A new orthonormal dither is then applied, and the algorithm iteratively applies a correction until the on-axis signal is maximized. The convergence time of the SPGD algorithm is proportional to the number of input fibers and inversely proportional to the dither frequency. For these experiments, frequency dithers of up to 100 kHz were used.

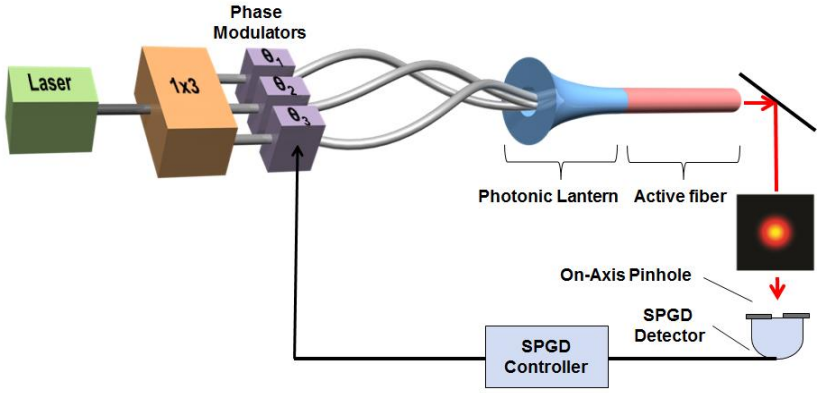

Fig. 4. Photonic lantern coherent combining schematic. The seed laser output is sent to a 1x3 splitter. The output of the splitter feeds an array of phase modulators. The output of the modulator array is input to a three-channel photonic lantern. The photonic lantern is mode matched to a three-moded gain fiber. The on-axis component of the output beam is sampled by a SPGD detector. The SPGD controller iteratively adjusts the input phases to maximize the on-axis intensity.

The SPGD signal along with a representative mode before and after the SPGD is turned on is shown in Fig. 5 below. When SPGD is turned off, the output of the fiber is generally a random superposition of higher-order modes. Shown on the top left of Fig. 5 is a single-frame image of the output of the fiber with SPGD off; the output beam resembles the LP11 modes with an on-axis null. When SPGD is turned on, the on-axis intensity is maximized, and the SPGD signal rapidly increases. The gain in the fiber was set to produce 0.5 W of output power. A low gain value was used in order to maintain a low level of backward emission so as to prevent damage to the phase-modulators and connectorized fiber connections. We anticipate that inserting isolators after the phase modulators and splicing all fiber components will allow increased output power. The output beam is observed to converge to the LP01 mode as shown in the upper right of Fig. 5. Furthermore, since the SPGD signal increases, CBC increases the brightness of the output as anticipated.

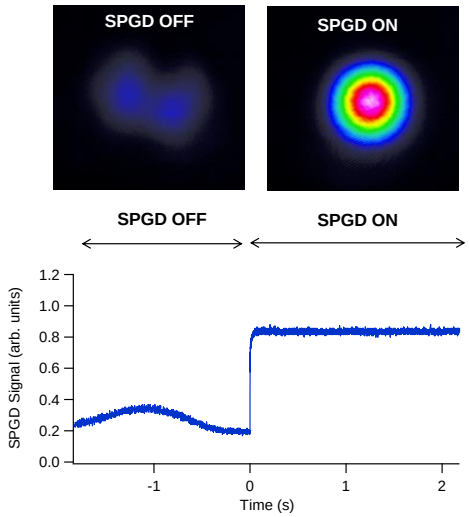

Fig. 5. Top (Left): Representative mode profile with SPGD off. Top (Right): Output mode with SPGD on. Bottom: SPGD detector signal measuring the on-axis intensity. An increase in the on-axis intensity occurs when SPGD is turned on at time equals zero.

In order to further quantify the performance of the photonic-lantern ASMC we performed modal analysis of the output with a spatial light modulator (SLM) using a correlation filter method [18-20]. The desired mode to be analyzed was projected onto the SLM. The multiplication of the incident field with the SLM pattern results in a correlation in the far field. The on-axis component of the far field provides the appropriate modal weighting intensity. The resulting modal decomposition from these measurements is shown in Fig. 6. This modal decomposition was taken from the photonic lantern output that was spliced into a passive 25/400 fiber prior to being spliced into the gain fiber.

As shown in Fig. 6 a random time-varying phase of the individual inputs to the photonic lantern result in a time-varying superposition of incident modes before SPGD is turned on. Once SPGD is turned on, the on-axis component rapidly increases with the end result of achieving a 97% combining efficiency into the fundamental mode. This result is consistent with our expected combining efficiency loss resulting from applying a phase-only correction.

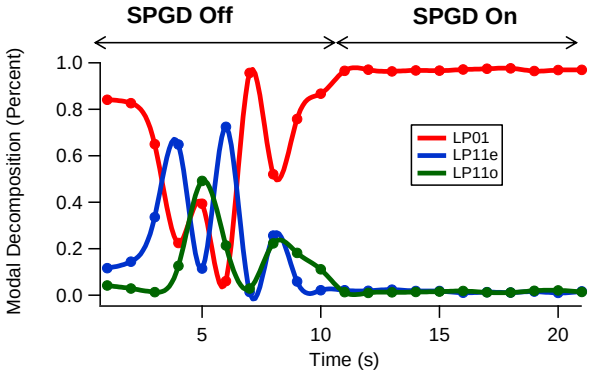

Fig. 6. Modal decomposition of the output of the photonic lantern spliced to a passive 25/400 fiber before and after SPGD is turned on. SPGD combines the power in the fiber into the LP01 mode.

This experiment was repeated after the photonic lantern was spliced into the gain fiber. At output power levels of 0.5 W, the modal decomposition resulted in all of the power being

delivered to the fundamental mode within the accuracy of our modal decomposition (estimated to be about ~ 1%). We attribute the slight increase in performance due to the improved modal overlap of the fundamental mode with the doped core, which provides additional modal discrimination.

4. Conclusions

We have demonstrated ASMC with a photonic lantern using SPGD. In this respect, the photonic lantern functions as an all-fiber-based adaptive optic. Namely, it enables coherent combination of input fibers at the seeding stage of an amplifier to achieve a diffraction-limited beam on the output.

Our results based on a few-mode (N=3) fiber are traceable to N>>3. Scaling requires that the number input modes on the photonic lantern match the number of modes in the delivery fiber. Coiling may serve to further reduce the number of modes, and photonic lanterns with over 120 channels have been developed offering promise toward even larger modal-area scaling [22].

Since the SPGD algorithm is a control algorithm that does not require *a priori* knowledge of the desired phase distribution, the particular disturbances that describe the mode coupling within the delivery fiber are irrelevant to the operation of the controller. This approach shows promise and has implications toward combating MMI arising from mode coupling at kHz rates. By implementing a control algorithm that works faster than the disturbance time-scale, it may be possible to eliminate the instability ultimately allowing continued scaling of the modal area and power of an individual fiber amplifier.

Acknowledgments This work is sponsored by the HEL-JTO under Air Force Contract #FA8721-05-C-0002. Opinions, interpretations, conclusions and recommendations are those of the author and are not necessarily endorsed by the United States Government.